SHIELDING OF SUPERCONDUCTING COILS FOR A 4-MW MUON-COLLIDER TARGET SYSTEM*

R.J. Weggel[†], N. Souchlas, Particle Beam Lasers, Inc., Northridge, CA 91324, USA
H.G Kirk, H.K. Sayed, BNL, Upton, NY 11973, USA
X. Ding, UCLA, Los Angeles, CA 90095, USA
V.B. Graves, ORNL, Oak Ridge, TN 37830, USA
K.T. McDonald, Princeton University, Princeton, NJ 08544, USA

Abstract

The target system envisioned for a Muon Collider/Neutrino Factory [1] features a liquid Hg jet target immersed in a 20-T solenoidal field. Field quality limits intercoil gaps to $\approx 40\%$ of the O.D. of the flanking coils. Longitudinal sag of the tungsten shielding vessels limits their length to ≈ 7 m. Support members adequate to resist intercryostat axial forces require an aggregate cross section of ≈ 0.1 m^2; the cryogenic heat leakage may be large. The innermost shielding vessel wall can be adequately cooled by helium gas only if its pressure is ≈ 10 atm and its velocity is ≈ 200 m/s. However, the analysis in this paper found none of these engineering challenges to be insurmountable.

GEOMETRY OF COILS & SHIELDING

Figure 1 sketches (in pink) a longitudinal, vertical section of the first dozen superconducting (SC) coils in the target-magnet design IDS120k. Every cryostat has three coils. Cryostat #1 begins at $z \approx -3$ m and ends at $z \approx 4$ m (where the downstream end of the beam/jet interaction region is at $z = 0$); subsequent intercryostat gaps are at spacings of 5 meters.
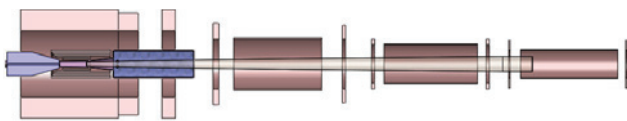

Figure 1: Longitudinal, vertical section of coils in design IDS120k.

Figure 2 sketches a longitudinal, vertical section of components inside, and in the bore of, Cryostat #1. Outermost is a set of three coaxial SC coils (cryostat not shown). Next is a shielding vessel consisting of two coaxial stainless-steel (SS) tubes capped by flanges, with tungsten beads as the shielding material. Inside, toward the downstream end, is another shielding vessel. Upstream of the midplane is a resistive magnet consisting of five nested coils that adds ≈ 5 T to the ≈ 15 T from the SC coils.
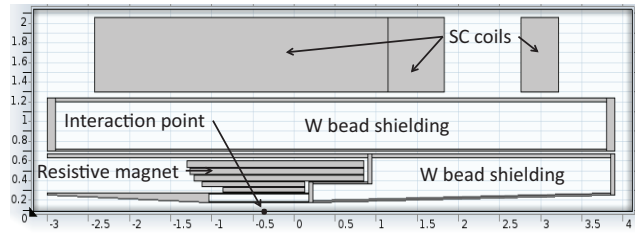
Figure 2: Longitudinal, vertical, upper half section near the proton-beam/Hg-jet interaction point. Distances are in meters.

QUALITY OF ON-AXIS FIELD PROFILE

Figure 3 plots the on-axis field profile. Despite very large intercoil gaps, the on-axis field differs by only a few percent from the desired profile.
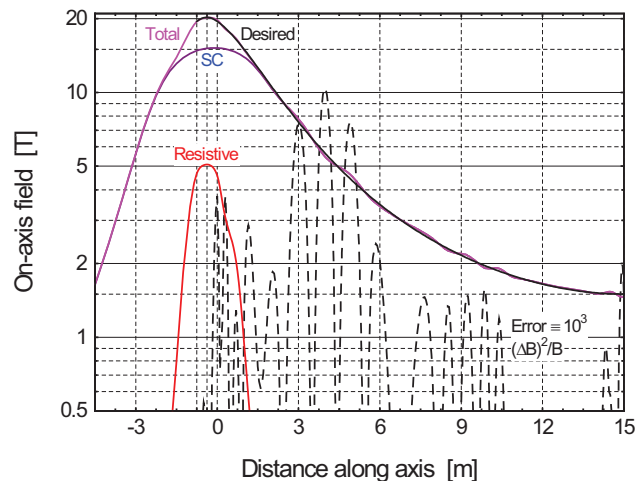

Figure 3: On-axis field profile of the SC coils, resistive magnet, and total field. The field deviations (dashed curves) from a desired profile are plotted as $10^3(\Delta B)^2/B$.

SAG IN SHIELDING VESSELS

The preferred material with which to fill the interior of the shielding vessels is tungsten, because of its density and
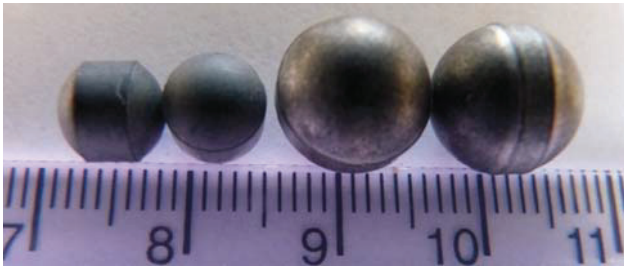
Figure 4: Tungsten (right) and tungsten-carbide beads.

high atomic number. The likely geometry is beads, in view of their abundant cooling surface and ability to fill all crannies of a vessel. Figure 4 shows beads of cobalt-bonded tungsten-carbide of density 14.5 g/cm^3 (left), and tungsten of 97% purity and density 18.2 g/cm^3 (right).

Experimental verification with marbles in water found their packing factor to be 61-62%. Beads of density 16.2 g/cm^3 would pack to a density of 10 g/cm^3. With such beads the outer shielding vessel would weigh nearly 200 tons; the inner vessel would weigh about 20 tons.

During some steps of assembly or removal for replacement, vessels must be supported from only their upstream end. Figure 5 plots the deflection *vs.* length for each of the vessels when so supported. To limit the sag to 4 mm, the outer vessel should be no longer than 8 m.

The shielding vessels not only sag along their length, they also bulge under the weight of their shielding beads, and due to internal pressure if cooled by helium gas at 10 atm. Figure 6 shows side views of the outer shielding vessel of Fig. 2, and (bottom) both its outer and inner tubes. The von Mises stresses and deformations (magnified 200-fold) are modest: $\sigma_{vM} < 107$ MPa; $\delta < 2.7$ mm). Some bulging is evident.
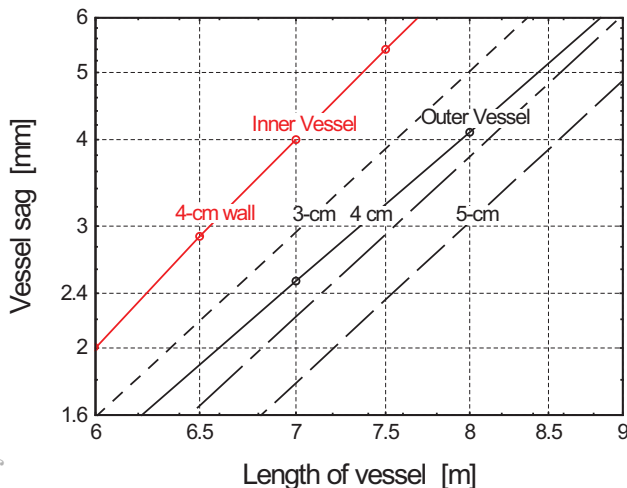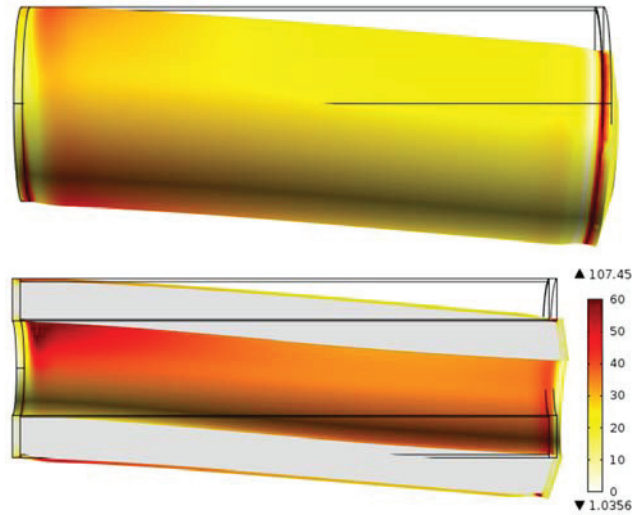

Figure 6: σ_{vM} & δ in outer shielding vessel of Cryostat #1.

AXIAL LOADS BETWEEN COILS

Table 1 lists the axial forces F_z in MN on each coil (Cu or SC) from either: 1) a triplet of SCs in any one of five cryostats; or 2) all coils = the 5-coil, 11-MW copper magnet plus the 18 SC coils in Cryostats #1 through #6. The largest magnetic forces on coils are those on SC #1 through #3; respectively, 534, -364 and -124 MN. (A minus sign indicates that the force points upstream.)

Table 2 summarizes the forces between cryostats from coils in one other cryostat or from all coils in the magnet.

Figure 5: Sag *vs.* length of shielding vessels, when cantilevered from one end.

Table 1: Forces F_z in MN on Each Coil From Each Coil Set

	Cryo. 1	Cryo. 2	Cryo. 3	Cryo. 4	Cryo. 5	All
Cu	0.721	0.102	0.0007	0.0001	0.0000	0.823
SC #1	519	11.1	0.0886	0.0168	0.0061	534
SC #2	-368	8.23	0.0366	0.0058	0.0019	-364
SC #3	-151	27.3	0.0567	0.0073	0.0021	-124
SC #4	-42.4	6.69	0.0796	0.0071	0.0018	-35.7
SC #5	-2.98	-2.61	0.168	0.0052	0.0009	-5.43
SC #6	-1.24	-4.07	1.69	0.0234	0.0030	-3.60
SC #7	-0.058	-1.14	0.670	0.0039	0.0003	-0.528
SC #8	-0.111	-0.766	0.151	0.220	0.0036	-0.502
SC #9	-0.0137	-0.0269	-0.821	0.634	0.0023	-0.225
SC #10	-0.0120	-0.0184	-0.722	0.511	0.0043	-0.237
SC #11	-0.0135	-0.0142	-0.130	-0.0004	0.129	-0.028
SC #12	-0.0044	-0.0031	-0.0053	-0.510	0.789	0.269
SC #13	-0.0037	-0.0024	-0.0033	-0.789	0.511	-0.283
SC #14	-0.0047	-0.0025	-0.0024	-0.129	-0.0011	-0.0109
SC #15	-0.0017	-0.0008	-0.0005	-0.0043	-0.511	0.271
Sum	-46.1	44.8	1.26	-0.0035	0.0219	0.0008

Table 2: Axial Forces F_z in MN Between Coil Sets

	Cryo. 1	Cryo. 2	Cryo. 3	Cryo. 4	Cryo. 5	All
Cu	0.721	0.102	0.0007	0.0001	0.0000	0.823
Cryo. 1	0.0040	46.6	0.182	0.0299	0.0102	46.1
Cryo. 2	-46.6	-0.0001	1.94	0.0356	0.0057	-44.8
Cryo. 3	-0.182	-1.94	0.0000	0.858	0.0063	-1.26
Cryo. 4	-0.0299	-0.0356	-0.858	-0.0001	0.922	0.0034
Cryo. 5	-0.0102	-0.0057	-0.0063	-0.922	-0.0009	-0.023
Sum	-46.1	44.8	1.26	-0.0035	0.0219	0.0008

The 534-MN force on SC #1 is nearly an order of magnitude greater than the 46-MN net force on its cryostat. This latter force points downstream (the compressive reaction force is on its downstream end), whereas the net force points upstream on Cryostats #2 & #3. The internal force within Cryostats #4 & #5 is tensile – each of its end coils is attracted more strongly to coils on the other side of its intercryostat gap than to the coils within its own cryostat.

VESSEL STRESSES & DEFORMATIONS

To withstand the force of attraction between Cryostats #1 & #2 requires structural members with an aggregate cross section $\approx$ 46 MN / 460 MPa = 0.1 m^2. Figure 7 plots the von Mises stress (σ_{vM}) and deformation (δ), magnified 100-fold, for bore tubes of 5-cm wall and flanges 10-cm thick, plus a SS bridge across the 93-cm gap between coils SC #2 & #3. Loads, distributed uniformly over the face of each flange, are given in the column "All" of Table 2. In both flanges of Cryostat #2 the maximum values of σ_{vM} and δ are $\approx$ 540 MPa and $\approx$ 5.5 mm, respectively. Analytic formulas [2] predict 350 MPa and 3.9 mm if both flanges share the load equally and the inner edge of each flange is "guided," *i.e.*, free to move axially but not radially.

The flanges in cryostats further downstream can be much thinner, because the axial force is at most 0.53 MN.
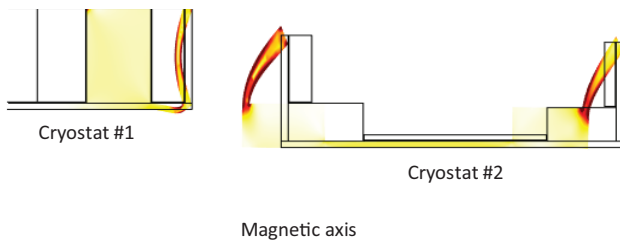

Figure 7: In Cryostat #2, σ_{vM} reaches 540 MPa; $\delta_{max} = 5.5$ mm.

HELIUM GAS COOLING OF BORE TUBE

The W shielding beads, and the vessels that contain them, will absorb $\approx$ 2.2 MW of the 4-MW proton beam power [3]. It is envisaged that helium gas, flowing at high speed, will be the coolant.

Helium gas is much poorer a coolant than water, which has an extraordinarily high heat capacity. However, He is preferable from the standpoint of minimal activation and chemical inertness. Helium flow will readily be capable of cooling shielding in the form of beads, which have ample surface area, provided the He does not heat up too much on its way from the inlet to the outlet of any shielding vessel. However, the inner wall of the vessel, which absorbs $\approx$ 400 kW, may be difficult to cool.

Figure 8 plots the deposited power density (DPD) *vs.* axial position in the vessel wall with the highest power density: the SS bore tube close to the interaction region. Each curve plots the DPD along a line of constant azimuthal coordinate. Along the solid red curve the DPD reaches 67 W/cm^3 [3] near $z = -20$ cm. An assumption of mirror symmetry about the plane $z = -20$ cm gives the solid black curve for the DPD in the region beyond that covered by the data file generated by the program (MARS15) that predicted the DPD. The integral under the curve is 3,400 W per cm of azimuthal extent for a bore tube of 1-cm wall thickness. A square-wave approximation to the curve has an axial extent of 3,400/67 = 50 cm.
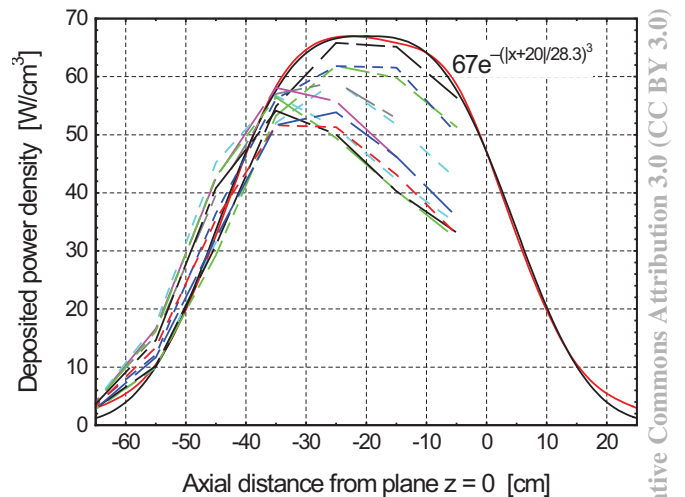

Figure 8: Deposited-power density in the beam pipe.

A computer model assessed the feasibility of cooling a slab with a uniform 67-W/cm^3 DPD and 50-cm length of heated zone. Cooling with helium gas turns out to be challenging. Even with a velocity of 210 m/s and pressure of 10 atm, helium can cool a bore tube only 9-mm thick, if cooling is from one side only and the temperature rise in the bore tube is limited to 80° C. The optimum depth of helium channel is 6 mm. The bulk, boundary-layer, and conduction temperature rises are 60° C, 18° C and 2° C, respectively. The hot-spot temperature rise in a bore tube 1-cm thick would be 92° C.

REFERENCES

[1] M.M. Alsharo'a *et al.*, *Status of Neutrino Factory and Muon Collider Research and Development and Future Plans*, Phys. Rev. ST Accel. Beams **6**, 081001 (2003).

[2] W.C. Young & R.G. Budygas, *Roark's Formulas for Stress and Strains*, 7th ed. (McGraw-Hill, 2002).

[3] N. Souchlas *et al.*, *Energy Flow and Deposition in a 4-MW Muon-Collider Target System*, WEPPD036, IPAC12.